

## Optical Spectropolarimetry of Broad Line Active Galaxies

M. E. Giannuzzo<sup>1</sup>, E. A. Corbett, A. Robinson, S. Young, J. H. Hough  
*Division of Physics and Astronomy, University of Hertfordshire,*  
*Hatfield HERTS AL10 9AB, UK*

D. J. Axon  
*Nuffield Radio Astronomy Laboratories, University of Manchester,*  
*Jodrell Bank, Macclesfield Cheshire SK11 9DL, UK*

**Abstract.** We present new optical spectropolarimetry of two bright type 1 AGNs. The observations are part of a project on broad line active galaxies in which, through data analysis and modelling, we aim to identify the polarization mechanism and to probe both the BLR and scattering region geometry and kinematics. The Seyfert 1 galaxy NGC 5548 and the radio galaxy 3C 445 display similar, and very interesting, structure across the broad H $\alpha$  line in their percentage polarization and position angle. The main features of the spectra are a polarization drop and a large angle swing, both strongly asymmetric with respect to the line center. The possible interpretations of this behavior, particularly in terms of the combination of two different scattering regions, are discussed.

### 1. Introduction

Spectropolarimetric observations of narrow line (type 2) AGNs have had a crucial role in developing unification theories, in which the differences between narrow and broad line (type 1) AGNs are explained by the partial obscuration of the central regions by a geometrically and optically thick torus (Antonucci & Miller 1985). Scattering models, in which the light from an obscured BLR and central continuum source is scattered into our line of sight by a cone-shaped scattering medium coaxial with the torus, successfully explain many of the polarization properties of type 2 AGNs (e.g., Young et al. 1995, Young et al. 1996). However, these models fail to reproduce the known polarization properties of type 1 AGNs, since they predict a polarization position angle orthogonal to the system axis (i.e., the projected radio axis), whereas most type 1 AGNs show a parallel alignment (Brindle et al. 1990).

The potential implications of this difference for unification theories led us to perform renewed high signal-to-noise spectropolarimetric observations of broad line AGNs, which have revealed a remarkable diversity in the properties of their broad Balmer lines. In some objects the H $\alpha$  line polarization is identical to that

---

<sup>1</sup>e-mail: email: ester@star.herts.ac.uk

of the continuum, while others exhibit complex structure with both the percentage polarization ( $P$ ) and position angle ( $\theta$ ) varying across the line. For example, in the two objects discussed here, 3C 445 and NGC 5548, both  $P$  and  $\theta$  change significantly from the red to the blue wing of the line profile. This behavior could favor radial flow over virial motions in the BLR, contrary to the conclusions of reverberation mapping studies of the latter (Peterson 1993). However, the geometry and kinematics of the scattering region may contribute substantially to the observed polarization features. Similarly, the polarization properties of some radio galaxies cannot be easily reconciled with current models for double-peaked  $H\alpha$  profiles (Corbett et al. 1998). Spectropolarimetry, therefore, is not only an important test of AGN unification theories, but can also provide information on the largely unknown structure and kinematics of the BLR and its scattering environment.

The most likely explanation for the different polarization properties of AGNs is that the dominant scattering and polarizing process takes place in different regions in type 1 and type 2 objects, the different geometries of which produce parallel polarization in the first case and perpendicular in the latter. The suggested cone-shaped scattering region could be responsible for the observed perpendicular polarization in narrow line AGNs, giving little contribution in broad line objects due to the small scattering angles involved. A scattering medium located closer to the BLR/continuum source, and therefore obscured by the torus in narrow line AGNs, could instead produce the type 1 parallel polarization if the gas has a toroidal or disk-like geometry, e.g., that of an ionized atmosphere of the obscuring torus facing the continuum source. The unique diagnostic strength of spectropolarimetry lies in the fact that the scattering regions provide a view of the central emitting source which can be different from that accessible to us, and it should be possible in principle to deconvolve the views to provide a better understanding of the geometries involved.

The particularly interesting polarization features of the two objects here discussed could possibly be interpreted in terms of both scattering regions contributing to the polarized emission. Neither of the objects in fact exhibits the close alignment between continuum polarization PA and radio axis typical of type 1 AGNs. To investigate qualitatively the viability of a two-component scattering geometry, we developed a simple model in which the observed radiation is the combination of different sets of Stokes parameters representing different components: a non-scattered, direct component which can be intrinsically polarized in the continuum, and two scattered components. The polarization of the latter is at different position angles, as a result of the different scattering geometries. This configuration, if allowing for wavelength shifts due to Doppler effects, can qualitatively explain the main observed features.

Section 2 summarizes the observations and data reduction, describes the model and its application to the observed data; section 3 includes a brief discussion on these preliminary results.

## 2. Observations, data reduction and model

The two spectra shown here (Figs. 1 and 2) were taken at the WHT 4.2 m telescope located in La Palma, in late June 1997; their dispersion is about 1.5 Å

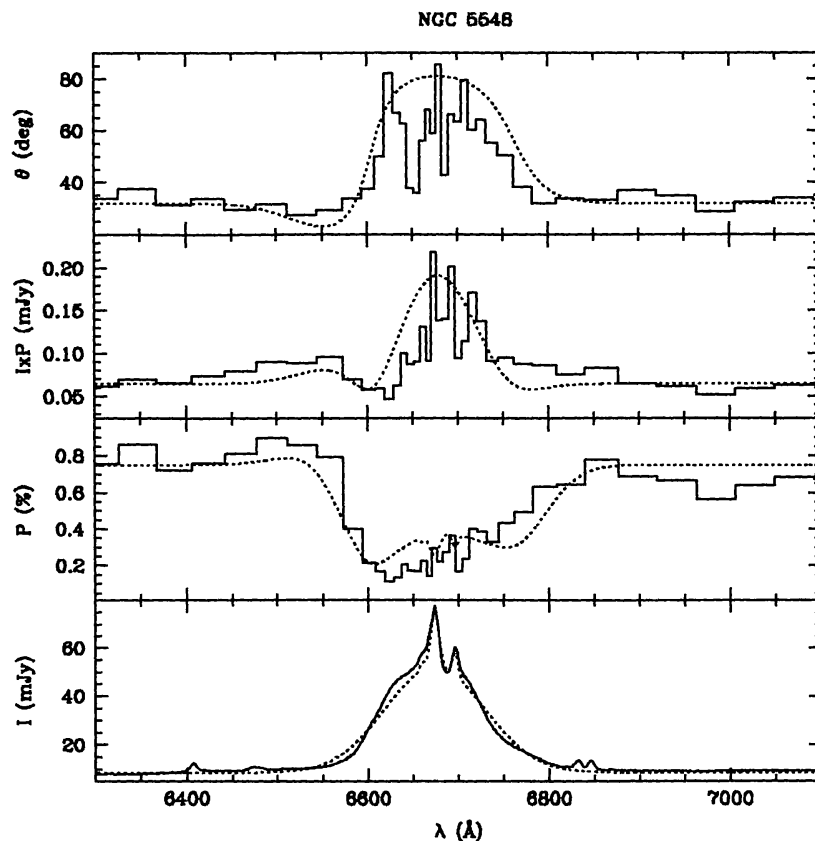


Figure 1. Spectropolarimetry data (solid line) and model results (dotted line) for NGC 5548.

$\text{pxl}^{-1}$  and the observations were performed according to standard spectropolarimetric techniques. The data reduction made use of standard tasks within the Starlink packages TSP and FIGARO (for more details on both observing and reducing techniques, see, e.g., Corbett et al. 1998).

Both objects display a misalignment between the continuum polarization PA and the radio axis ( $\sim 50^\circ$  in NGC 5548 and  $\sim 30^\circ$  in 3C 445). Furthermore, in both the line polarization is drastically lower than the continuum. This cannot be entirely explained by depolarization due to the narrow line emission (which is produced in a region co-spatial with or bigger than the scattering regions, and therefore undergoes little scattering), given the broad spectral range over which the line polarization drops. The continuum radiation, therefore, must include a polarized contribution which is not shared by the line emission, and which is thus probably intrinsic; it can possibly be associated with a contribution of synchrotron radiation to the thermal optical continuum. Furthermore, as already noticed there is a strong asymmetry in the polarization spectra of the objects: in both  $P$  drops steeply in the blue wing of the line but rises smoothly in the red wing; as a consequence, the line profile in polarized flux is almost entirely concentrated redwards of the line center and presents a very broad red wing.

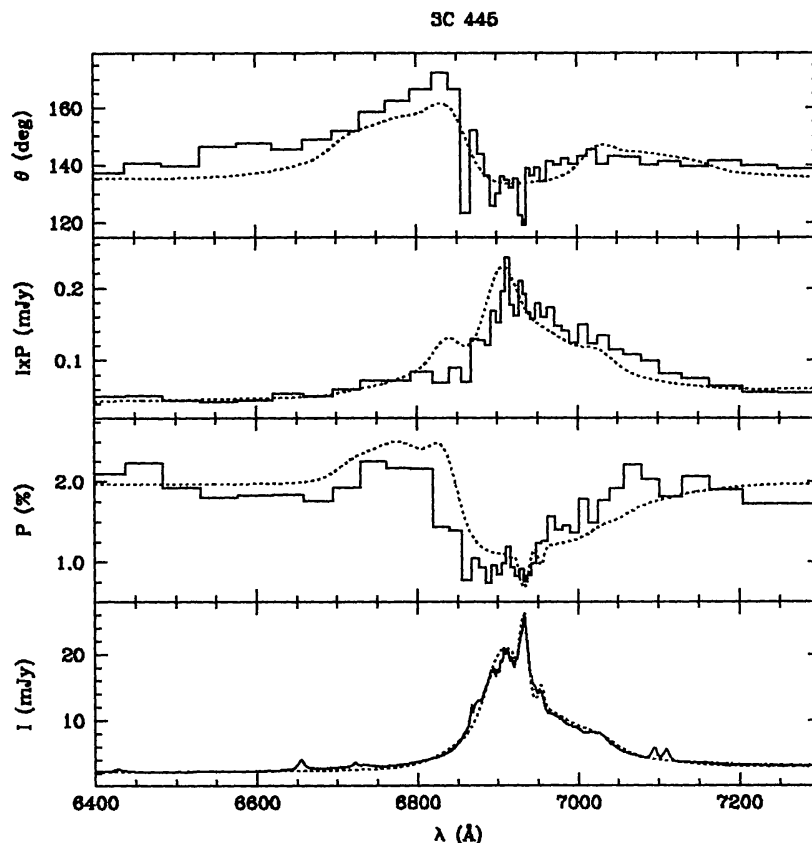


Figure 2. Spectropolarimetry data (solid line) and model results (dotted line) for 3C 445.

The wavelength dependence of the position angle, however, is quite different in the two objects. NGC 5548 exhibits two swings in PA over the line, the peak of the broader one coinciding with that of the polarized flux profile and the narrower one occurring in the blue wing of the line. By contrast, 3C 445 exhibits a broad swing in PA over the blue wing of the line, while little or no angle change is detected in the line center and red wing.

A simple code was developed to reproduce qualitatively the wavelength dependence of the polarization and PA observed in these sources. This code makes use of the property of additivity of the Stokes parameters and combines two scattered components with a non-scattered one to fit the observed line profiles. This non-scattered, or direct, component is associated with radiation escaping directly from the BLR and continuum source, and hence is itself a combination of two components: an emission line, represented by a multi-Gaussian fit to the observed line profile, and a continuum, modelled with a linear fit, of which some fraction is intrinsically polarized, as discussed above. The linear continuum parameters and its intrinsic polarization were determined from the observed spectra. The two scattered components were used to represent toroidal and conical scattering, and were therefore constrained to have polarization PAs aligned parallel ( $0^\circ = 180^\circ$ ) and perpendicular ( $90^\circ$ ) to the system axis respectively.

The free parameters in this model are the fractions (assumed to be wavelength-independent) of the direct line and continuum flux density scattered by each scattering region, and the wavelength shifts introduced into the scattered flux by the relative motion of the scatterers and BLR gas. We therefore assume that the scatterers see the same line profile that we do, but shifted in wavelength.

With these relatively simple and schematic assumptions we obtained a set of Stokes parameters for NGC 5548 which qualitatively reproduces that observed (Fig. 1). The best fit corresponds to a ‘perpendicular’ scattered component almost unshifted in wavelength ( $\sim 10 \text{ \AA}$ ) and representing a fraction  $\sim 0.6\%$  of the incident flux, and a weaker –  $\sim 0.3\%$  – ‘parallel’ component blueshifted compared to the line center of approximately  $60 \text{ \AA}$ ; the latter is thus responsible for the asymmetries observed in polarization and position angle. The continuum intrinsic polarization has  $P \sim 1\%$  and  $\theta \sim 22^\circ$ .

The same model, however, is not applicable to 3C 445, where the swing in  $\theta$  is not simply asymmetric, but entirely concentrated in the blue wing of the line, whereas the line profile, both in total and polarized flux, is strongly red-dominated. We had to assume, therefore, that in this case all or part of the scatterers have a view of the central source which differs from our own: this can happen, for example, if the profile asymmetry in total flux is related to orientation. We tested several hypotheses, among which were the possibilities that one of the scattering regions sees a ‘symmetrized’  $\text{H}\alpha$  profile (i.e., one with the blue wing identical to the observed red one) or a blue-asymmetric profile (i.e., a mirror image of the observed one, with a pronounced blue wing instead of a red one), or that only the broader line components are scattered. The only assumption which gave a result consistent with the observed spectra is that there exists a component of the ‘parallel’ scattering medium which sees a blue-asymmetric profile, as if having a sort of ‘complementary’ view of the BLR compared to the one we and the other scatterers have (Fig. 2). Here the main scattering component is not giving a perpendicular polarization, but polarization at a position angle close to the observed continuum one ( $\sim 130^\circ$  vs  $\sim 140^\circ$  for the continuum), and it represents a fraction  $\sim 1\%$  of the incident flux, again unshifted in wavelength. To a  $\sim 0.3\%$  parallel component redshifted by  $\sim 120 \text{ \AA}$  we added a second  $\sim 0.6\%$  parallel component blueshifted approximately by the same amount: this latter one is the result of the scatterers seeing a line profile dominated by a broad blue wing. The continuum intrinsic polarization has again  $P \sim 1\%$ , with  $\theta \sim 117^\circ$ .

### 3. Discussion

Though with our simple model it is not possible to reproduce the fine structures observed in the spectra, nor the exact shape of the polarization and position angle wavelength dependence, nevertheless a few important points have emerged from this investigation: firstly that the combination of different scattering components producing different polarization PAs may in principle explain the complex structures observed in the polarization spectra of some objects.

Secondly, it might be necessary to assume a small intrinsic continuum polarization, which suggests a contribution from synchrotron radiation even in objects in which the optical continuum is dominated by thermal emission.

According to these results, the scattering region producing parallel polarization, i.e., in our scenario the toroidal one, is subject to Doppler shifts in the two objects considered here, possibly due to high velocity motions of the scatterers located close to the BLR/continuum source. However, being difficult to disentangle this motion from that of the line emitting gas, the presence of radial motions in the BLR cannot be excluded. For example, the fact that in 3C 445 a part of the scatterers see a different profile – and the only approximate agreement with the data suggests that they actually see a more intense blue wing than we assumed, or a quite differently shaped profile – could be related, as already suggested, to the reason for the observed line profile asymmetry in total and polarized flux. A bi-conical radial outflow of proper geometry for the line emitting gas could possibly explain the blue/red asymmetries observed in the total flux and in the polarimetry data. The viability of these possibilities will be investigated in future work.

Finally, the closeness of the observed position angle of the continuum and the main part of the line in 3C 445 may be the result of the common (line and continuum) polarizing scattering mechanism: the intrinsic continuum PA is in fact more than  $20^\circ$  lower than the observed one.

Detailed scattering models, as the ones developed at the UH, will be applied to these data in the future, together with more physical total flux profile models, to provide a better understanding of the processes involved and of the geometry and kinematics of the various components.

## References

- Antonucci, R. R. J., & Miller, J. S. 1985, *ApJ*, 297, 621  
Brindle, C., et al. 1990, *MNRAS*, 244, 577  
Corbett, E. A., Robinson, A., Axon, D. J., Young, S., & Hough, J. H. 1998, *MNRAS*, 296, 721  
Peterson, B. M. 1993, *PASP*, 105, 247  
Young, S., Hough, J. H., Axon, D. J., Bailey, J. A., & Ward, M. J. 1995, *MNRAS*, 272, 513  
Young, S., et al. 1996, *MNRAS*, 281, 1206